Kovove Mater. 49 2011 319–331
DOI: 10.4149/km_2011_5_319

Application of acoustic emission to monitor bainitic and martensitic transformation

T. Z. Wozniak[1]*, K. Rozniatowski[2], Z. Ranachowski[3]

[1]*Institute of Technology, Kazimierz Wielki University, Chodkiewicza 30, 85-064 Bydgoszcz, Poland*
[2]*Faculty of Materials Science and Engineering, Warsaw University of Technology, Woloska 141, 02-507 Warsaw, Poland*
[3]*Institute of Fundamental Technological Research, Polish Academy of Sciences, Pawinskiego 5B, 02-103 Warsaw, Poland*

Received 20 October 2010, received in revised form 19 May 2011, accepted 1 June 2011

Abstract

The paper concerns acoustic emission (AE) measurements during isothermal martensitic and bainitic heat treatments in 100CrMnSi6-4 bearing steel. A distribution of the total RMS voltage in arbitrary unit (AU) during austempering together with the M_S temperature results was determined. M_S represents the temperature at which martensite starts being formed. This temperature was determined with the use of the dilatometric method. The Short Time Fourier Transform algorithm was used for displaying the signal values on spectrogram graphs. AE signals were attributed to a midrib. Midrib is a thin-plate isothermal martensite formed before lower bainite nucleation. The evolution of midribs in remaining austenite was investigated with AE measurements at the temperature near M_S. Macroscopic effects of elongation changes and their division into various intensity stages related to a martensite transformation were analyzed. A comparison of the AE curves and dilatometric results suggests that the AE method determines a relatively initial stage of the martensite transformation, during which additional processes of austempering and carbon partitioning occur. Lower bainite containing the midrib was found to evolve in two stages.

K e y w o r d s: bearing steels, phase transformation kinetics, acoustic methods, isothermal heat treatments, midrib, bainite

1. Introduction

Acoustic methods are widely used for gathering information on the properties and structure of materials and underlying processes occurring at the source. Acoustic emission (AE) is a phenomenon in which elastic waves are generated due to rapid release of strain energy from localized sources within a material [l–3]. Both longitudinal and transverse elastic waves can be generated by an abrupt local force. A unified explanation of the AE source has not been provided yet, but it is usually considered as a process which involves plastic deformation (dislocation movement), crack growth, phase transformations (bainitic and martensitic) [4–10]. Strongly localized processes during the phase transition lead to the formation of significant shear and dilatation strains, which produce the main AE source. When the austempering temperature approaches the M_S temperature, the transformation rate rapidly increases [11, 12]. M_S represents the temperature at which the formation of martensite will start. This acceleration is a result of the rapid formation of midribs during early stages of austenite decomposition. A midrib is thin-plate twinned martensite which allows AE to be observed using special research techniques [9, 10]. Midrib formation is also related to the swing back effect in the bainitic transformation kinetics. Although the nature of the midrib is still not fully understood, it has been concluded that a midrib thin plate is the first area of bainite sheaves [11–14]. The mechanism of bainite formation has been the subject of numerous original research papers and reviews. There is very little literature concerning the AE method applied in bainitic transformation invest-

*Corresponding author: tel.: +48-52-341-91-08; fax +48-52-341-47-73; e-mail address: wozniak@ukw.edu.pl

igations as well as the use of this technique as an argument for this transformation to be explained by a displacive mechanism. The AE technique is competitive in many aspects.

The basic objective of this work is to study AE induced by the evolution of a midrib in remaining austenite during the isothermal transformation as well as the microstructure of lower bainite with a midrib. A unique method for recording signals of the AE was developed. In order to conduct austempering and to record acoustic effects that occur during the process, a special stand was designed. For the control of heat treatment processes, this method requires untypical, original set-ups and a special software. This kind of treatment has been applied, among others, in the bearing industry [15, 16]. Implementation of new heat treatment schemes that are based on martensitic and bainitic transformations requires a strict control of processed elements in order to provide high quality steel. The suggested treatment method is based on phenomena that occur in high-carbon steels at the temperature near the M_S which is typical of so-called 'swing back in kinetics' [11, 13]. The present invention relates to new control methods of heat treatment for bearing steel components.

2. Research methodology

2.1. Material and composition dependences

The experiments were conducted using 100CrMnSi6-4 steel (EN ISO 683-17:1999). The chemical composition analysis was performed with the use of a Spectrolab analyzer. The results are presented in Table 1. The material, used for production of rings and rolling parts of bearings, shows high purity at low sulphur content (0.007 wt.% S), and consequently, relatively few MnS inclusions. The investigated steel was delivered as rolled bars in a softened state, 46 mm in diameter, from the same casting batch. Due to a 1.5 % chromium addition, the 100CrMnSi6-4 steel is highly hardenable. If silicon and manganese are introduced, hardenability of big-sized bearings (e.g. rings of thickness > 30 mm) can be obtained. Bearing steel, apart from manganese which improves hardenability, also contains silicon. In the presence of carbide formers, silicon improves steel hardenability and its plastic properties in the austempered state. The Si effect is only effective if a sufficient amount of Si is present [17]. The 0.57 % level of the investigated steel is not sufficient to prevent cementite formation, but the effect of Si on transition carbide formation is not fully understood.

The heat treatment used for the AE experiments is illustrated in Fig. 1. The experiments were based on heating to the temperature of 950 ℃ by holding for 30 min and quenching to the bainite holding temperature

Table 1. Chemical composition of steel (wt.%)

C	Mn	Cr	Si	Ni	Mo	S	P
0.95	1.10	1.47	0.57	0.07	0.01	0.007	0.014

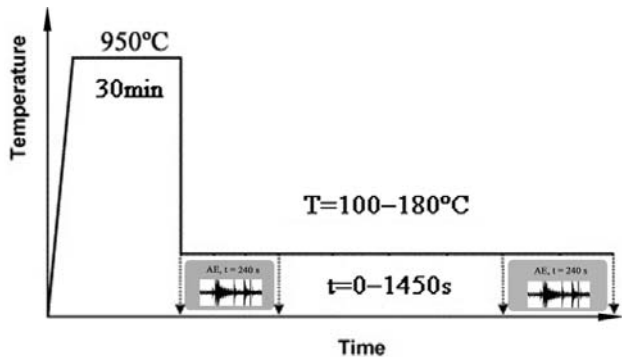

Fig. 1. Illustration of the heat treatment during the experiment conducted in the AE measurement set-up with marked time intervals between results recording.

ranging from 30 ℃ to 190 ℃ for 1240 s followed by quenching to room temperature.

For calculations of the martensite-start temperature M_S, the relationship (1) in the form of a simple linear equation [8] was used:

$$M_S(℃) = 462 - 273x_C - 26x_{Mn} - 16x_{Ni} - \\ - 13x_{Cr} - 30x_{Mo} \quad (1)$$

with the concentration x in wt.%.

To calculate the volume fraction of martensite f_m as a function of temperature, the K-M equation (2) was applied [17, 18]:

$$f_m = 1 - \exp(-\alpha_m(M_S - T)), \quad (2)$$

where α_m is the rate parameter. The composition dependence of the rate parameter α_m was described by a simple linear equation (3), similar to the well-known Andrews' empirical relationship between M_S and composition [8], as:

$$\alpha_m(K^{-1}) = 0.0224 - 0.0107x_C - 0.0007x_{Mn} - \\ - 0.00005x_{Ni} - 0.00012x_{Cr} - 0.0001x_{Mo} \quad (3)$$

with the concentration x in wt.%.

Different carbon contents in remaining austenite x_γ were calculated by:

$$x_\gamma = \bar{x} + V_b\frac{\bar{x} - x_\alpha}{1 - V_b}, \quad (4)$$

where V_b is the volume fraction of lower bainite with a midrib, $\bar{x}$ is the overall amount of carbon in the steel.

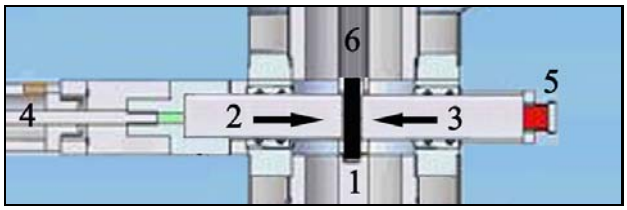

Fig. 2. An illustration of a part of the experimental set-up: the specimen (1), the movable waveguide (2, 3) moved towards the specimen, pneumatic servo-motor (4), wide band differential AE sensor WD (5), a transporting mechanism of the tested specimen in oil (6).

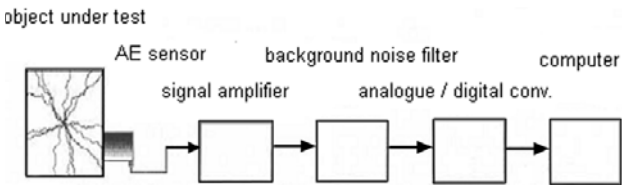

Fig. 3. A block diagram of the experimental set-up used for the AE measurement.

In the calculations, a simplification of the amount of carbon trapped in the bainitic x_α as 0.3 % was assumed [19].

In the TTT diagram for the 100CrMnSi6-4 steel, slightly enhanced transformation near the M_S temperature was observed [20, 21]. In particular, it should be expected to influence AE effects.

The AE specimens were examined using light metallographic methods in order to demonstrate the existence of bainite and martensite in the transformed sample. The microsection etching was performed by means of a Nital reagent. The specimens were austenitized at a temperature of 950 ℃ for 30 min with a data recording precision of 5 ℃, which resulted in dissolution of a significant amount of carbide in austenite. Fully austenitized samples were rapidly cooled down to various temperatures range between 30 ℃ and 190 ℃. Subsequently, they were held at that temperature over a specific time period in order to partially transform the austenite into bainite. The isothermal transformation was interrupted once the AE signals disappeared. During the further cooling, the remaining austenite transformed partially to martensite.

2.2. Experimental setup and measuring procedure

AE can be observed using a special setup (Figs. 2, 3), within the temperature range of isothermal martensite transformation 30–190 ℃. The experiment was conducted on cylindrical specimens (1) with a diameter of 45 mm and a thickness of 2 mm. After austenitization, they were inserted into a specially designed transporting mechanism (6) (setup) in oil. The transformation measured by AE was delayed by about 2 s due to transportation of specimens. An acoustic sensor (5) was installed previously on one of the two movable mandrels (2, 3) serving as a waveguide and connected to an analyzer [9, 10]. Signals were recorded by means of an AE analyzer 10/20 kHz – 800 kHz. Surface displacements were measured with a wide-band (100–1000 kHz) differential AE sensor (PAC model WD). The root-mean-square (RMS) value of the background noise V_n at the preamplifier input was approximately 12–15 μV. The best setting for low power AE signals corresponded to the total amplification of 66 dB (×2000) in the 0.01–0.8 MHz band. The cut-off frequency of the high-pass filter was 20 kHz. The filter was used in order to reduce the background thermal noise during further processing. During the measurement reproducibility testing, with the identical source and the same sensor mounting, the standard deviation was 4 % per 30 measurements. Each data point represents the average of at least 5 measurements.

Owing to the file size restrictions which resulted from high frequency of sampling, two ways of signal analysis were applied. The first one consisted in using signal digital analysis with sampling rate at 1.2 MHz, which limited maximum recording time of isothermal heat treatment process to 240 s. The results of digital processing enabled us to apply event detection, determine the AE event signal energy, prepare spectrogram and apply the digital filtration technique. According to ASTM E1316-05, the AE event means local material change that gives rise to an acoustic emission. The AE signals were analyzed with the use of special software. The AE signals from the amplifier output were transmitted to the analyzing system with the use of the ADLINK 9812. Although the system resolution was 0.8 μs, considering the applied algorithm of event detection, the accuracy of the event meant three signal samples, i.e. 2.4 μs. According to ASTM E1316-05, the parameter count gave the number of times the AE signal exceeded preset threshold level during any selected portion of a test. The algorithm analyzed digital signal samples in a 2–2048 scale (for a physical range of 0–5 V).

The second way of signal analysis consisted in the use of RMS voltage signals with time constant 0.1 ms. This method enabled us to study AE activity during an isothermal heat treatment process that lasted 5000 s. For that purpose a microprocessor was used to add up all RMS voltage signals that occurred in turn during every second with sampling frequency 10 kHz. The sum total of RMS voltage signals per each second was registered in the processor memory, in a scale: 0–1000, which were defined as arbitrary units (AU). It means that a maximal result of the sum total of RMS signals per second can amount to 10^7 (in units of AU). AE activity was characterized by a rate AE parameter

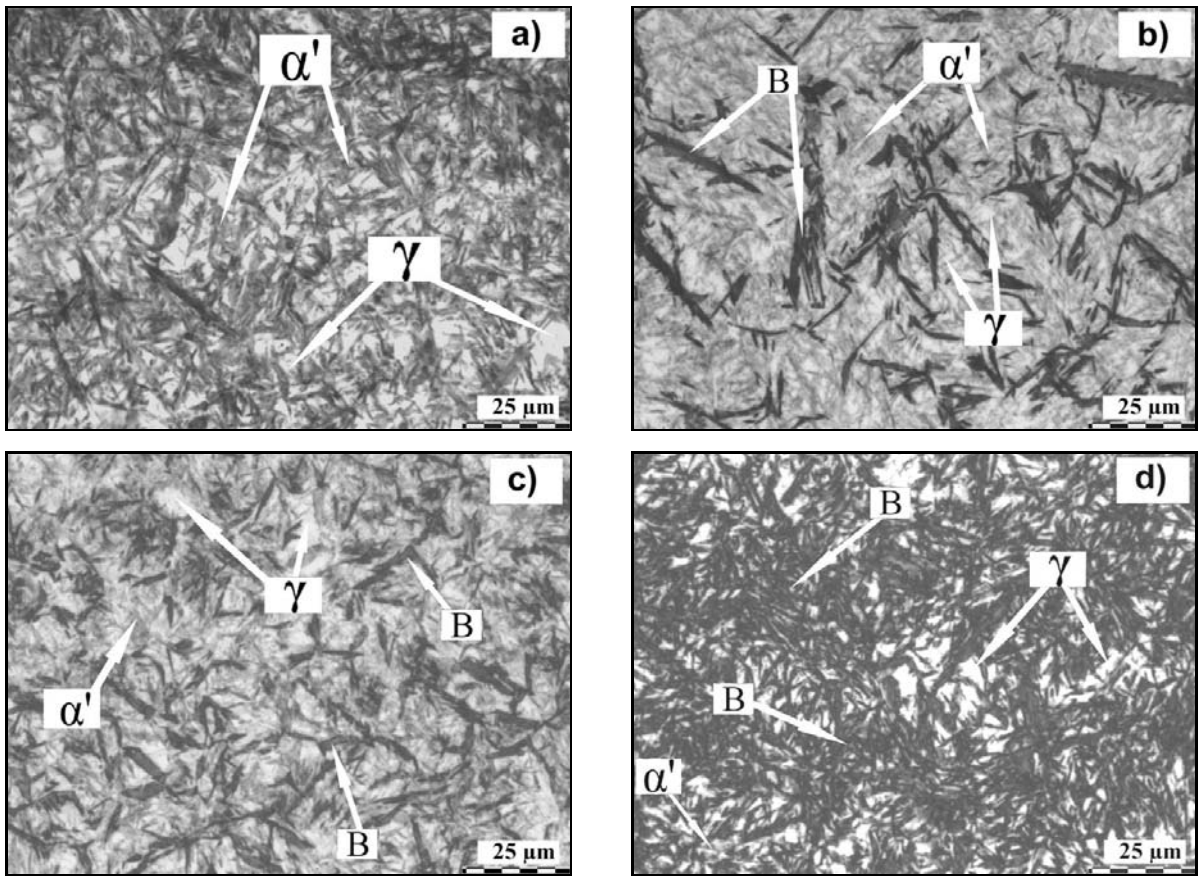

Fig. 4. Light microscopic pictures of the specimens after austempering at different temperatures: a) 100 ℃, b) 130 ℃, c) 160 ℃, d) 180 ℃; etching with Nital reagent, holding time: 1450 s. The symbols α', B, γ stand for martensite, bainite and retained austenite, respectively.

AU vs. time. The mean square voltage $\overline{V^2}$, corrected for the background noise (AE power), is defined by [6]:

$$\overline{V^2}(t) = \frac{1}{\tau}\int_{t}^{t+\tau} V_{\mathrm{t}}^2(t')\mathrm{d}t' - \overline{V_{\mathrm{n}}^2}, \tag{5}$$

where $V_{\mathrm{t}}(t')$ is the voltage output at the transducer, τ is a time constant 0.1 ms, V_{n} is the value of the background noise level.

The M_{S} temperature of the steel was measured with the use of an Adamel Lhomargy LK 02 dilatometer. Cylindrical specimens 12 mm in length and 2 mm in diameter were heated to 950 ℃, and then rapidly cooled. Formation of martensite during cooling was detected for six specimens. For theoretical determination of M_{S} temperatures, simple linear equations were applied [8].

3. Results

3.1. Microstructure of isothermally transformed specimens

The isothermal transformation led to formation of different phases identified in the micrographs: martensite, bainite, retained austenite and transition carbides ε, which could not be distinguished by light microscopy. A majority of carbides at 160 ℃ in bainitic ferrite are sized up to 10 nm. Obviously, the technique does not allow for distinguishing details in various etching areas. Also, plate martensite forms are generally too fine to be differentiated in the light microscope, but a shape of martensite is clearly revealed. Even though light microscopy cannot analyze structure in detail, it is easy to distinguish bainite from martensite and to observe lower bainite with a midrib and even a midrib in bainite sheaves. In a simple light microscope, the microstructure of bainite appears darker than martensite due to its low reflectivity. The bainite etches dark because it is a mixture of ferrite and carbide, and the interfaces are easily attacked by applied Nital etchant. Figure 4 shows some of the light metallographic pictures, obtained after the bainite holding time of 1450 s at the temperature range between 100 ℃ and 180 ℃. The light-grey areas in Fig. 4a represent retained austenite γ, while martensite is shown in the others. It is seen that γ retains in blocks.

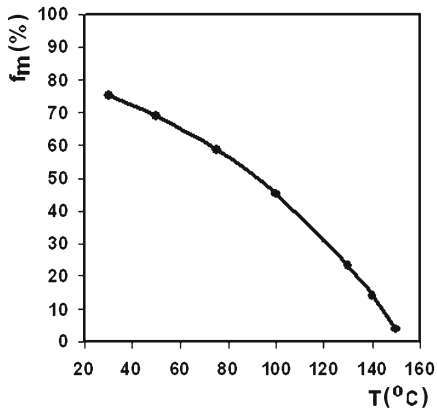

Fig. 5. The results of changes in the volume fraction of martensite f_m as a function of the temperature, calculated with the use of the K-M equation.

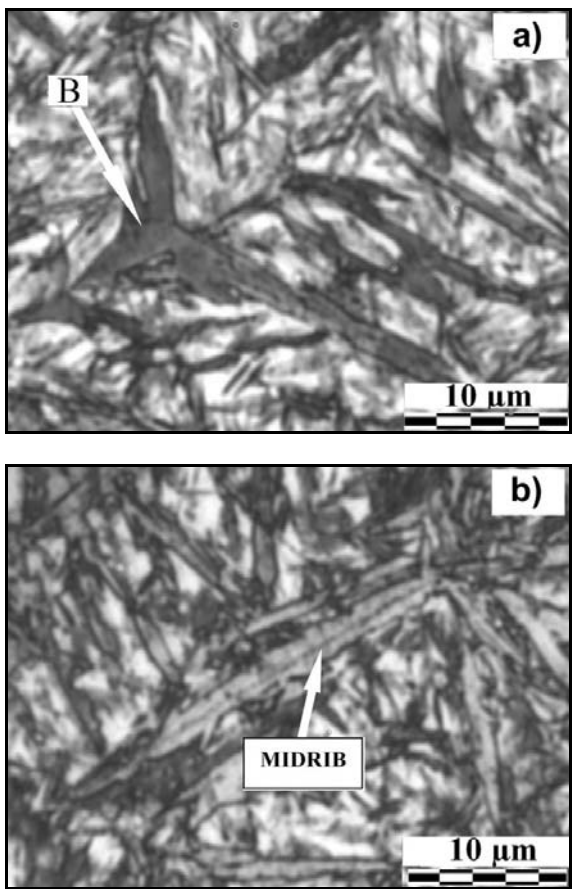

Fig. 6. Selected fragments of the structural elements after austempering at 160 ℃: a) butterfly bainite – B, b) midrib in the centre of the sheaf; α' – the areas of athermal martensite that undergoes transformation when cooled down to the room temperature.

The theoretical martensite-start temperature M_S can be somewhat lower than experimental, depending on the austenitizing treatment and especially on carbon concentrations. In the experiments described here, an austenitization temperature of 950 ℃ was chosen, leading to dissolution of a significant amount of carbides. Thus, the effect of the austenitization temperature rise is a decrease in the M_S temperature. In the calculations of the volume fraction of martensite as a function of the transformation temperature (Fig. 5), a constant value $\alpha_m = 0.013$ was assumed in the K-M equation (2). In practice, the α_m coefficient value depends on the carbon content, which changes during the transformation. The carbon enrichment in austenite at temperatures near M_S would lead to a greater reduction in the volume fraction of martensite that formed midribs. This was confirmed by the results of metallographic examination where midrib fraction in the microstructure was observed after the isothermal transformation at 130–160 ℃ (Fig. 4b,c), which accelerated bainite transformation. In the micrographs, distinct sheaves of lower bainite with a midrib (Fig. 6) were observed. The specimen's microstructure consists of bainite (black 'needles'), martensite and retained austenite in blocks. Microstructural observations of bainite confirmed a number of plates of butterfly morphology containing midribs. Formation of the butterfly shape is preceded by formation of two intersected or twisted midribs that are thin-plate martensite.

The micrograph of the specimen after holding at 130 ℃ quantitatively shows that the fraction of bainite is significantly increased. Bainite plates of the butterfly morphology dominated in the microstructure at the first stage of the transformation. At the second stage of the reaction, the lenticular bainite was formed, generally nucleating on the grain boundaries. At 130–160 ℃, it is seen that γ_R retains the morphology of film type and it less frequently occurs in blocks. The type of retained austenite (γ_R), located between bainitic ferrite plates, is very fine and stable due to enrichment with carbon. In the light metallographic pictures, due to the fine structure, it is difficult to distinguish the film-type morphology of the retained austenite. Based solely on the metallographic research of larger bainite volume fractions, it is difficult to establish whether the observed sheaves show the presence of lenticular bainite or bainite with a midrib [22]. These differences may be only revealed in an electron microscope. The earlier electron micrographs showed light trail-shaped midribs [11] after austempering in the bainite with a midrib. The carbon concentration at the centre of bainite plate (where the midrib should be located) was always lower than the average solute level in the alloys.

Austenite contained about 0.57 wt.% of silicon which inhibited cementite precipitation, but the level of Si was insufficient to prevent cementite formation. Therefore, the remaining austenite was enriched with carbon to some extent during bainite formation (Fig. 7). The bainite transformation must stop when

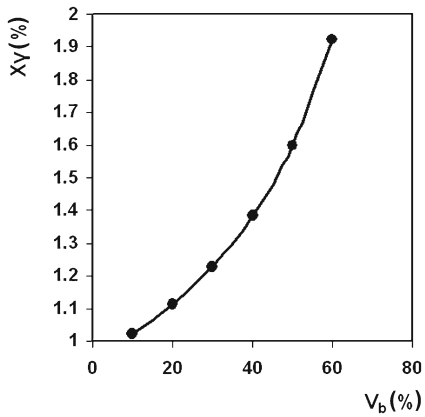

Fig. 7. Calculation results of the enrichment of the remaining austenite with carbon x_γ for a partial transformation of austenite into lower bainite with a midrib V_b, using a constant value of the amount of carbon trapped in the bainitic x_α as 0.3 %.

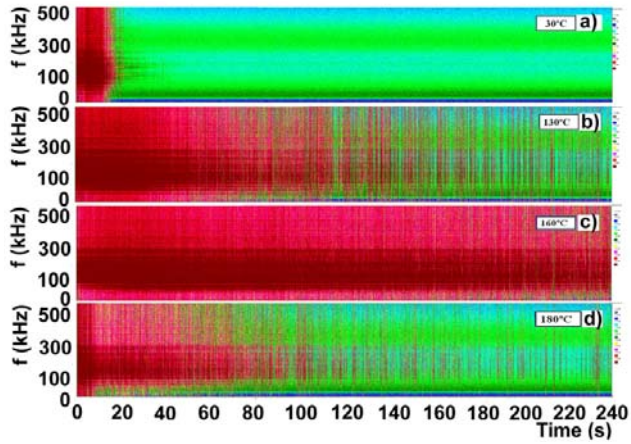

Fig. 8. Spectrograms of the AE signals for 100CrMnSi6-4 steel, after austempering at: a) 30 °C, b) 130 °C, c) 160 °C, d) 180 °C. The x-axis indicates the signal recording time (240 s), the y-axis – the frequency of the recorded signal in the linear scale of 0–600 kHz. The colours encode the root values of the power spectral density of the recorded signal in a 9-grade scale. The lowest signal power is marked dark-blue (light), and the highest – dark-red (dark).

the enrichment of remaining austenite with carbon corresponds to that given by the T_0' curve [23]. The T_0' curve is the locus of all points on the temperature versus carbon concentration plot where austenite and ferrite of the same chemical composition have identical free energies, taking into account the stored energy of the ferrite due to the displacive mechanism of transformation. It would be expected that during the bainite formation, the transformation into a midrib in the remaining austenite occurred gradually with increasing carbon content, which led to the process inhibition as the consequence.

3.2. Acoustic emission measurements

For spectrogram preparation, the Short Time Fourier Transform (STFT) algorithm with the Hamming window was used [24]. The software has a graphics window for displaying maximum power of signal values in consecutive time frames of 15 milliseconds each. A single frame is obtained from 17640 signal samples. The next 1647 samples inside the frame where the signal had the highest value were used for calculating the spectrum. Sample spectrograms of the AE signals, obtained during austempering, are presented in Fig. 8. The increase in the austempering temperature causes prolongation of single AE events, which is the effect of overlapping isothermal martensite plates. A lower austempering temperature results in a higher AE power spectral density of events only at the beginning of the process.

The AE testing results are shaped by many factors related with the emission in the tested source and with the detection in a transducer used for this testing. The AE system consists of the transducer that converts an elastic transient displacement into a voltage signal followed by a signal conditioning system. A frequency pass-band of the applied integrated system is between 20–800 kHz. Signal parameters usable to make quantitative analysis are: power and energy, determined in the whole spectral range, but limited by the band-pass filter used for this research. In order to find spectral line with maximal values, the computing results of the AE signal RMS values for selected frequencies (50 kHz, 75 kHz, 150 kHz, 200 kHz, 300 kHz, 400 kHz) were used. The AE signal RMS values were calculated using the digital filtration technique. Figure 9 presents representative runs of RMS signals within the 200 kHz frequency band where the investigated phase transition processes had the maximum power. In order to define the spectral range where the power achieves maximum, RMS values of AE signals versus RMS values for 400 kHz were calculated, and are shown in Fig. 10. To achieve a more clear shape of line in the presented figure, the curve for the selected frequencies (200 kHz/400 kHz) was recorded in a form of the trend line as a movable average for 10 pixels, but for the other signals – as a movable average for 100 pixels.

The analysis of the AE event signal energy was performed using specially designed software. This software analyzed AE events that exceeded the background noise level. In the measurement procedure, an AE event was established to be recorded when a signal value exceeded the discrimination level of established 1000 mV, with the maximum signal value of 5000 mV. In order to eliminate signal disturbances from the group of true events, the sum of two previ-

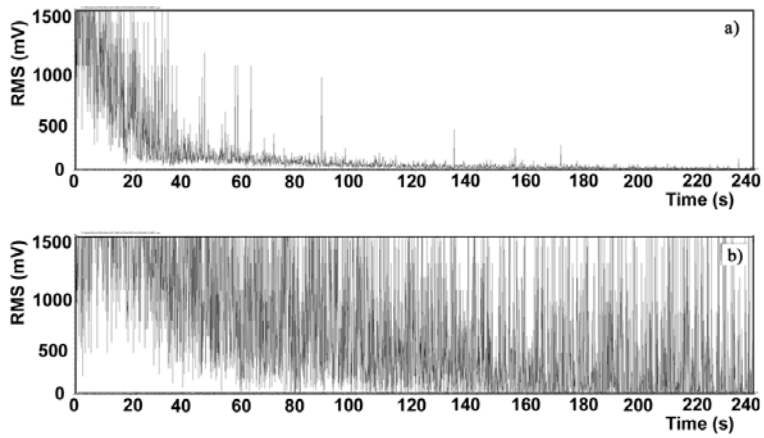

Fig. 9. The course of the RMS values of the signals, within the 200 kHz frequency band in which most of the energy during the investigated phase transition processes was emitted, during austempering at: a) 100 ℃, b) 160 ℃.

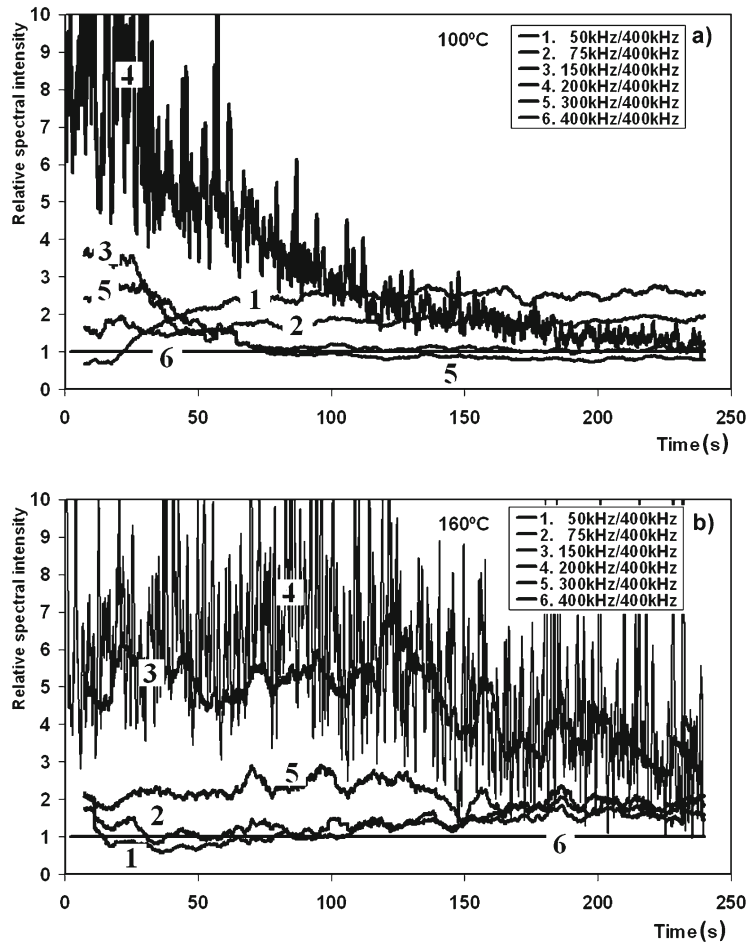

Fig. 10. The courses of the RMS values of the AE signal for selected frequencies versus the 400 kHz frequency band ((1) 50 kHz/400 kHz, (2) 75 kHz/400 kHz, (3) 150 kHz/400 kHz, (4) 200 kHz/400 kHz, (5) 300 kHz/400 kHz) for the 100CrMnSi6-4 steel, after austempering at: a) 100 ℃, b) 160 ℃.

ous samples was subtracted from the sum of two neighbouring samples in the procedure. When the difference exceeded 1000 mV, an event start was signalized and it was timed until the next difference got smaller than 1000 mV. The AE event signal energy was calculated as 1/2 a squared value of the maximum amplitude of the signal multiplied by the event duration. Changes in the AE event signal energy (in pJ) generated during

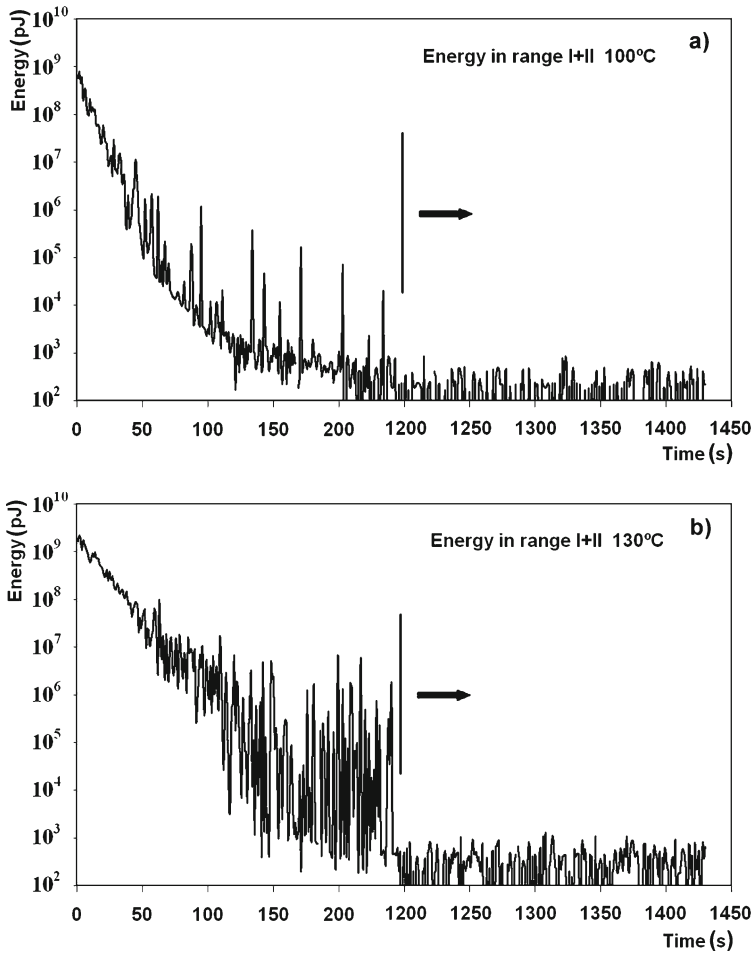

Fig. 11a,b. The comparison of the AE event signal energy calculated for each consecutive time slice of 1 s at the beginning and after 20 min of the isothermal transformation process at: a) 100 ℃, b) 130 ℃.

austempering, for various transformation conditions, are presented in Fig. 11. In view of the technological capability of the software and long duration of the AE in the analyzed cases, the AE event signal energy analysis was performed both for the first 4 min and after 20 min of austempering at 100–180 ℃ (the second stage of the AE event recording, marked with an arrow in Fig. 11).

The results of the AE measurements, performed at lower quenching temperatures (presented in Figs. 8a–11a), indicated a very short time of the isothermal martensitic transformation. The essential emission effects were found in the time range of up to 50 s (spectrograms in Fig. 8). Afterwards, the transformation occurred locally with single AE events. At that time, the AE event signal energy (calculated in time slices of 1 s) was reduced by 4 orders of magnitude, and eventually, after 100 s, it was equal to the energy of background noise (Fig. 11a).

Within the temperature range of 100 ℃ to 180 ℃, a gradual shift in the duration of intense emission was observed (Figs. 9–11). The AE event signal energy measurement results, obtained during the first 4 min of recording (presented in Fig. 11), showed an abrupt character of transformation, during which the events with relatively high energy occurred. In the next stage at 130 ℃ (stage No. II in the period of 1200–1450 s) the AE event signal energy was reduced to the background level, while in the same stage but at 180 ℃, a few signals with high energy appeared. At 130 ℃ and 180 ℃, there were some similarities in the dependence illustrating energy changes (Fig. 11b,d). When the temperature achieved 160 ℃, intense isothermal martensitic transformation occurred. It is clearly seen in the spectrogram (Fig. 8) as an explicit acoustic beam with the longest duration. The dominant spectral range was still within 100 kHz – 300 kHz. The enhanced acoustic activity was confirmed by other results as well. In Fig. 9b, at that temperature, the intensity of the RMS signals for 200 kHz was so high that it occupied the whole window space in regard to duration of signals. The results for the AE event signal energy at 160 ℃ were also very high for both recording stages I and II, as shown in Fig. 11c. During the first 4 min, the signals were so intense that the curve illustrating energy change was continuous. No single

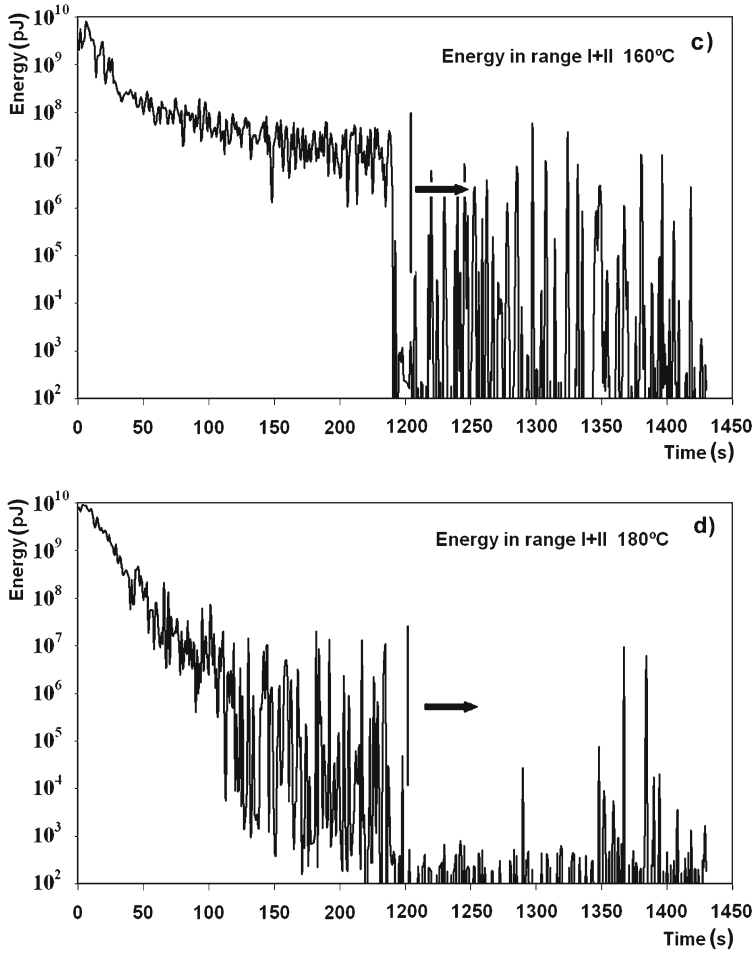

Fig. 11c,d. The comparison of the AE event signal energy calculated for each consecutive time slice of 1 s at the beginning and after 20 min of the isothermal transformation process at: c) 160 °C, d) 180 °C.

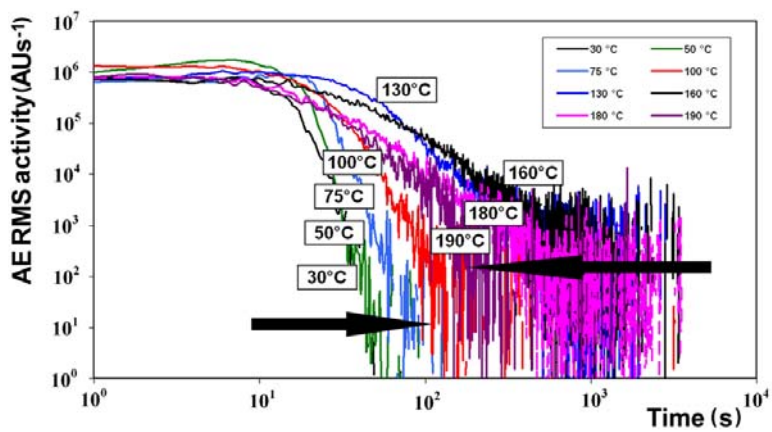

Fig. 12. The dependence of a rate AE parameter AU vs. time for different austempering temperatures at 30–190 °C. Parameter AU denotes sum of the AE RMS voltage of the signals in arbitrary unit (AU) per second.

AE event could be detected over this period. Their number gradually decreased with the increase in the transformation time at 160 °C. The AE event signal energy during the stage II at 160 °C was still as high as the energy in the stage I (240 s) at 130 °C. The results of the present study indicate that the number of martensite plates that formed midribs, increase at the transformation temperature of 160 °C.

On the curves of AE RMS activity as a sum of voltages (in arbitrary unit AU) per second, a char-

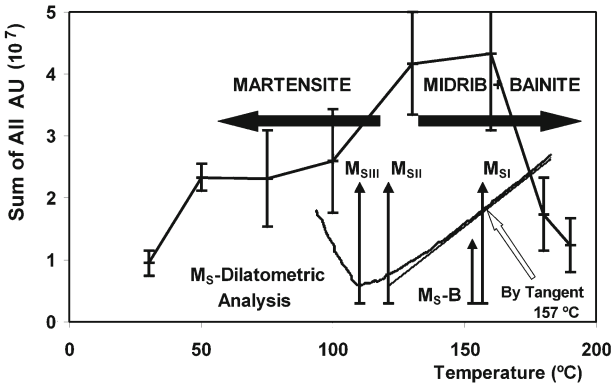

Fig. 13. A distribution of the AU sum total (axis-Y) during austempering including the results achieved at M_S temperature by using dilatometric method. The figure also presents the M_S calculation result obtained with the use of Bohemen's (Ms-B) [5] equation.

acteristic peak was observed at the time of approximately 10 s for all cases, which was followed by a decrease. As the temperature increased from 30 to 130 ℃, curve shifts to longer times were noted. Above 130 ℃, as the temperature increased to 190 ℃, curve shifts in opposite direction to shorter times were observed (Fig. 12). Based on the results of the AE RMS activity at various temperatures, the sum of all AU was calculated (Fig. 13). At lower temperatures, the sum of all AU was stable. Next, it increased within 130–160 ℃ to a maximum, followed by a fast drop. A maximum range of the AU sum total comparable to that observed at 160 ℃ also occurred at 130 ℃. Despite the fact that both the longest AE time occurred and a maximum range of the AU sum total was observed at 160 ℃, the time corresponding to 50 % of the AU sum total, comparing to all temperatures, was delayed. At 160 ℃, 95 % of the AU sum total was completed until elapsing the time of approximately 450 s. With reference to 130 ℃, 95 % of the AU sum total was completed just after approximately 110 s [25].

On a dilatometric curve, detected by high-resolution dilatometric analysis, the non-isothermal austenite-to martensite transformation did not occur in one single stage (Fig. 13). This transformation splitted into different and successive stages limited by different points M_{SI} – M_{SIII}. The martensite transformation start temperature ($M_{SI} = 157$ ℃) was determined as the temperature at which the thermal contraction, shown by the dilatometric curve, deviated from linearity due to the volume expansion associated to the martensite transformation. As indicated in the diagram, the principal martensitic transformation M_{SIII} (massive austenite-to-martensite) was identified by a minimum in the curve. $M_{SII} = 121$ ℃ represents the temperature at which the splitting below M_{SI} commences.

4. Discussion

4.1. Swing back phenomenon in the remaining austenite transformation

The M_S temperature calculations, based on known mathematical relationship, gave a result within 130–160 ℃. The temperature increase to 180 ℃, i.e. above the M_S, resulted in a large reduction in the rate of bainitic transformation, initiated by the produced midribs. In the micrographs, distinct sheaves of lower bainite with a midrib (Fig. 6) were not observed at 180 ℃. This is a result of a relatively large volume fraction of new reaction products. The time of midrib formation is significantly prolonged, which is confirmed by longer acoustic activity. Hence, the true M_S temperature can be assumed to approach the upper part of the C-curve nose that explains the kinetics of midrib formation.

The previously described characteristic features of the microstructure correlate with the intensity of the AE which was higher when the temperature of austempering was closer to 130–160 ℃. At such temperatures, a maximum AE activity and a maximum range of the AU sum total, induced by the formed midribs, were observed. AE activity can relate to interfacial migration between ferrite and austenite during martensitic transformations. Atomic displacements, associated with glissile boundaries, were highly ordered and led to large strains. The product of the dislocation glide distance and velocity determined the amplitude of the AE [26, 27].

The maximum rate of midrib formation was related to the acceleration of bainitic transformation. This appeared to occur due to the development of carbon-rich and carbon-poor regions in the residual austenite where the bainitic transformations were initiated [28]. The lower bainite containing midribs subdivided the region of austenite, which resulted in a refinement of the austenite grain size and, consequently, a refinement of the bainite during the subsequent transformation of austenite. The matrix in light grey is the martensite and retained austenite, as shown in Figs. 5a,d.

The analysis shows that the rate of decomposition was higher if isothermal transformation occurred in the range of swing back in kinetics [22]. The results of microstructural studies allowed for the assumption that at 130–160 ℃, the C-curve nose was observed, which determined a relatively large volume fraction of bainite. A fine microstructure consisting of bainitic ferrite and film-type austenite gives an excellent combination of strength and toughness in high-Si steels because the retained austenite can act as an additional obstacle for crack propagation [29]. For years, most researchers who specialize in martensite field have focused on a transformation process during continu-

ous cooling. In the majority of TTT diagrams, S- or C-curves are observed. The studies suggest that each type of transformation product, as well as isothermal martensite [20, 21], has a separate C-curve. There is an extensive evidence about the 'Swing Back' phenomenon [11, 13, 30]. It is a distinct austenite decomposition acceleration just near the M_S below the nose of the bainitic transformation. The 'Swing Back' phenomenon near the M_S is, in reality, the upper shoulder of the C-curve of the isothermal martensitic transformation start. In the TTT diagram, determined by Davenport and Bain [31] for a lower temperature range (100–200 ℃), a C-curve was observed that represented the kinetics of isothermal martensitic transformation. The diagram became a dominant tool for a description of the kinetics of overcooled austenite isothermal decomposition. In late 1940s and early 1950s, Kurdjumow and Maksimova [32] discovered the isothermal martensitic transformation. Supporting Davenport and Bain [31], they thought that the amount of martensite might increase with time at a constant temperature. In some steels, both martensite types (twinned plate and lath) may form simultaneously, while in others they have separate C-curves. Zhao and Jin [20] reviewed the TTT diagrams, for which the data below the M_S were also obtained.

Earlier, some contribution towards the explanation of this phenomena was made by Radcliffe and Rollason [33] using the electrical resistance measurement method. Also, on the basis of dilatometric and microstructural studies on 0.85–1.8 wt.% carbon steels, an acceleration of the transformation start was confirmed near the M_S temperature in approximately up to 25 % of bainite volume fraction [11, 34]. Bainite nucleation occured on so-called midribs.

4.2. Acoustic emission induced by the evolution of midribs and carbon partitioning

At 180 ℃ that exceeds the M_S, the effects of AE are induced by forming bainite and tempering (Fig. 13). In the second stage of the experiment, the emitted signals are rare, but their energy is very high. Therefore, the acoustic picture presented in the spectrogram (Fig. 8d) is less intensive contrary to the previous ones. At higher isothermal heat treatment temperatures, low emission may be linked to the pinning of the quenched-in dislocations by very small carbides. Precipitates both within and on the boundaries between laths provide additional impediments to quenched-in dislocations. AE is believed to originate from the propagation of high velocity ($> 100\ \mathrm{m\,s^{-1}}$) dislocation groups, too. About 40 dislocations, moving simultaneously, are required to give a detectable signal [26, 27, 35]. Then, their signals are in the same phase and their amplitudes sum up. Such cooperative motion requires an existence of the mechanism to coordinate the slip, so this mechanism cannot generate AE here. At 100 ℃, the microstructural features (Fig. 4a) as well as the energy distribution curves and spectrograms (Figs. 8a and 11a) prove that the emission signals are induced by formation of athermal martensite plates and their rapid growth.

Recently, an alternative process designed to control the fractions of martensite and retained austenite, named Quenching and Partitioning (Q&P), has been developed. It involves quenching to the martensite-start temperature (M_S), followed by ageing either at or above the initial quenching temperature. During the bainite transformation, carbon is partitioned into residual austenite after the diffusionless growth of each bainite plate. The austenite can only transform into bainite if carbon concentration is smaller than a value given by the T_0' curve. In the regions where the carbon concentration is higher, midribs can form if the conditions determined by Oka and Okamoto are met [11]. As a result, a growth in the transformation rate of bainite occurs due to formation of the martensite plates of a midrib morphology [11, 13, 30, 36].

Q&P may not operate in these alloys as the Si levels are insufficient to prevent cementite formation, hence martensite tempering is likely to compete with carbon partitioning (Fig. 13). The splitting into different stages in Fig. 13 is also caused by the concentration gradients produced in the austenite by the diffusion of carbon from dissolved carbides during heating. M_{SI} point corresponds to the volume increase that occurs during the midrib formation in areas of austenite poor in carbon and carbide-forming elements. A weak intensity of this effect indicates that it is a result of the martensitic transformation of small amounts of austenite. This type of splitting is generally explained in terms of carbide precipitation during cooling [37]. At the M_{SI} 157 ℃, determined as the dilatometric curve deviation from the straight line, a maximum AE activity was observed. The more expansion anomaly identifying M_{SII} 121 ℃ stage indicates that it is also associated with a partial martensitic transformation of areas of austenite less concentrated than the massive austenite. At 190 ℃, despite large numbers of total AU, the splitting is not observed yet. A certain lack of full correlation between AE and dilatometric results is also affected by a time factor. Emission effects were investigated under isothermal conditions but dilatometry measurements – during continuous cooling.

For several years, studies on high-strength steels containing the low temperature bainite and significant amounts of interlath retained austenite have been developed [19]. As the blocky type of retained austenite has usually a larger grain size than the film-type austenite, enrichment of the film-type austenite with carbon is expected to be higher than in the blocky type [29, 38]. Carbon partitioning in martensite and residual austenite is typically omitted in customary

quenched steels because oversaturation of martensite with carbon is usually eliminated by carbide precipitation during tempering. Therefore, the chemical composition of retained austenite does not typically differ from the average chemical composition of steels.

The intensity of AE signals is highly sensitive to microstructure. Defects of the structure are attributed to the shear transformation mechanism. The shape strain causes plastic deformation which, in turn, leads to a relatively large dislocation density in both the parent and product phases. Other kinds of defects, such as twinning and faulting, are also found in the residual austenite. These accommodation defects are common in martensitic transformations if the IPS shape change cannot be elastically accommodated. There is, however, a significant difference as bainite grows with relatively small driving forces. Defects induced by bainitic transformation do not seem to play as crucial a role in stimulating further nucleation as it happens with plate martensite. Although some excessive carbon is retained in the ferrite solution in bainite, after transformation most of it is partitioned into the residual austenite.

The growth rate of martensite can be so fast as to be limited only by the speed of sound in the metal. Although bainite grows rapidly, the lengthening rate is much smaller than that for martensite. The interface moves relatively slowly even though it is glissile. This is probably because of the plastic work that is done as the bainite grows. Carbide precipitation influences the reaction rate by removing carbon either from the residual austenite or from the supersaturated ferrite [39].

The micromechanism of AE does not seem to be connected with dislocation-precipitate interactions. Single dislocations are shown to be incapable of generating detectable AE [35], and carbide precipitates do not constitute significant disturbances for propagation of ultrasonic waves. As the acoustic wavelength is considerably larger than average grain sizes, Rayleigh scattering occurs. The microstructure parameters that affect ultrasonic attenuation values are the average volume of grains and the elastic anisotropy coefficient [40].

5. Conclusions

The main objective of this work was to study AE induced by the evolution of midribs in austenite over the holding time during the isothermal transformation and the microstructure of the lower bainite with a midrib.

1. The AE method can be successfully applied with regard to 100CrMnSi6-4 steel in order to monitor and control the kinetics of transformation. During the isothermal martensitic transformation, the longest process of midrib formation occurs at 160 ℃, while the shortest and most intense one at 130 ℃, which is also observed in spectrograms. It is a result of the formation of many midribs over the first 50 s.

2. The origin of AE effect lies in the understanding of interfacial migration between ferrite and austenite during a martensitic transformation. Splitting into different stages during a martensite transformation is caused by concentration gradients produced in the austenite as a result of carbon diffusion. These concentration gradients originate from dissolved carbides during heating and martensite tempering, likely to compete with carbon partitioning. The development of carbon-rich and carbon-poor regions in the supercooled austenite and the evolution of carbon content in residual austenite are one of the main challenges in understanding a bainitic transformation near the M_S in bearing steels.

3. At 160 ℃, with the elongation of the bainitic transformation, the AE event signal energy (generated per second) does not significantly change, contrary to the event rate. The analysis of acoustic activity at this temperature and the microstructural analysis allow for the assumption that above the M_S, along with the increase in the austempering temperature, the rate of midrib formation diminishes. It may be a result of the thermodynamic driving force reduction and a decrease in enrichment of the remaining austenite with carbon due to carbide precipitation as the Si level is insufficient to prevent cementite formation.

4. Regardless of the temperature change, the dominant spectral power range is constant within 100–300 kHz. The maximum spectral power occurs within the frequency range of 150–200 kHz. The determination of this range is possible with the use of the relative spectral intensity RMS of the signals.

5. The AE method, used in the study of bainitic and martensitic phase transformation, provides a useful tool for controlling the phase constituents in 100CrMnSi6-4 bearing steel. It is a real time detection technique that can be used to study processes that involve shear, dilatation and a rapid release of the strain energy. Further work is necessary in order to determine the kinetics of midrib formation as well as the influence of the processing on tempering that is likely to compete with carbon partitioning. The application of AE to study transformation behaviour is a valuable technique to supplement dilatometry.

Acknowledgements

This work was carried out with financial support from the Polish Ministry of Science and Higher Education under project number R15 010 02. The authors wish to acknowledge Prof. Krzysztof J. Kurzydlowski MSc, PhD from the Faculty of Materials Science and Engineering, Warsaw

University of Technology, for providing the research equipment, and Prof. Jerzy Jelenkowski MSc, PhD from Warsaw Institute of Precision Mechanics for valuable discussions. It is a pleasure to acknowledge Mikolaj Poplawski PhD from the Institute of Materials Science and Engineering, Poznan University of Technology, for assistance with the dilatometric measurements, Olga Rochowska-Siwiec MA and Tomasz Dzikowski MA for good cooperation.

References

[1] WADLEY, H.—SCRUBY, C.—SPEAKE, J.: Int. Metals Rev., *25*, 1980, p. 41.
[2] SPEICH, G.—SCHWOEBLE, A.: Acoustic emission during phase transformation in steel. In: Monitoring Structural Integrity, ASTM STP 571, 1975, p. 40.
[3] RICHETON, T.—WEISS, J.—LOUCHET, F.—DOBROŇ, P.—CHMELÍK, F.: Kovove Mater., *45*, 2007, p. 149.
[4] BOHLEN, J.—CHMELÍK, F.—KAISER, F.—LETZIG, D.—LUKÁČ, P.—KAINER, K. U.: Kovove Mater., *40*, 2002, p. 290.
[5] MEZA-GARCIA, E.—DOBRON, P.—BOHLEN, J.—LETZIG, D.—CHMELIK, F.—LUKAC, P.—KAINER, K. U.: Materials Science and Engineering A, *462*, 2007, p. 297.
[6] VAN BOHEMEN, S. M. C.—HERMANS, M. J. M.—DEN OUDEN, G.—RICHARDSON, I.: J. Phys. D: Appl. Phys., *35*, 2002, p. 1889.
[7] VAN BOHEMEN, S. M. C.—HERMANS, M. J. M.—DEN OUDEN. G.: Materials Science nad Technology, *18*, 2002, p. 1524.
[8] VAN BOHEMEN, S. M. C.—SIETSMA, J.: Metall. Mater. Trans. A, *40A*, 2009, p. 1059.
[9] WOZNIAK, T. Z.—RANACHOWSKI, Z.: Archives of Acoustics, *31*, 2006, p. 1.
[10] WOZNIAK, T. Z.: Materials Characterization, *59*, 2008, p. 708. doi:10.1016/j.matchar.2007.06.004
[11] OKA, M.—OKAMOTO, H.: Metall. Trans. A, *19A*, 1988, p. 447. doi:10.1007/BF02649258
[12] ZHI-GANG, Y.—HONG-SHENG, F.: Current Opinion in Solid State and Materials Science, *9*, 2005, p. 277.
[13] WOZNIAK, T. Z.: Materials Science and Engineering A, *408*, 2005, p. 309. doi:10.1016/j.msea.2005.08.148
[14] VAN BOHEMEN, S. M. C.—SANTOFIMIAA, M.—SIETSMA, J.: Scripta Materialia, *58*, 2008, p. 488.
[15] SPEER, J. G.—RIZZO, F. C.—MATLOCK, D. K.—EDMONDS, D. V.: Materials Research, *8*, 2005, p. 417.
[16] CHAKRABORTY, J.—BHATTACHARJEE, D.—MANNA, I.: Scripta Materialia, *59*, 2008, p. 247. doi:10.1016/j.scriptamat.2008.03.023
[17] KOISTINEN, D. P.—MARBURGER, R. E.: Acta Materialia, *7*, 1959, p. 59. doi:10.1016/0001-6160(59)90170-1
[18] VAN BOHEMEN, S. M. C.—SIETSMA, J.—HERMANS, M. J. M.—RICHARDSON, I. M.: Acta Materialia, *51*, 2003, p. 4183. doi:10.1016/S1359-6454(03)00236-2
[19] CABALLERO, F. G.—BHADESHIA, H. K. D. H.—MAWELLA, K. J. A.—JONES, D. G.—BROWN, P.: Materials Science and Technology, *18*, 2002, p. 279. doi:10.1179/026708301225000725
[20] ZHAO, J.—JIN, Z.: Metall. Mater. Trans. A, *8A*, 1992, p. 1004.
[21] JI-CHENG, Z.—MICHAEL, R.: Materials Science and Engineering R, *15*, 1995, p. 135.
[22] WOZNIAK, T. Z.: Archives of Materials Science, *23*, 2002, p. 351 (in Polish).
[23] GARCIA-MATEO, C.—BHADESHIA, H. K. D. H.: Materials Science and Engineering A, *378*, 2004, p. 289.
[24] PAWELEK, A.—KUSNIERZ, J.—JASIENSKI, Z.—RANACHOWSKI, Z.—BOGUCKA, J.: Archives of Metallurgy and Materials, *54*, 2009, p. 83.
[25] WOZNIAK, T. Z.: Archives of Foundry Engineering, *10*, 2010, p. 189.
[26] SKALSKYI, V. R.—ANDREIKIV, O. E.—SERHIENKO, O. M.: Materials Science, *39*, 2003, p. 86. doi:10.1023/A:1026182630649
[27] WADLEY, H.—SCRUBY, C.: J. Mater. Sci., *26*, 1991, p. 5777. doi:10.1007/BF01130115
[28] BABU, S. S.—SPECHT, E. D.—DAVID, S. A.—KARAPETROVA, E.—ZSCHACK, P.—PEET, M.—BHADESHIA, H. K. D. H.: Metall. Mater. Trans. A, *36A*, 2005, p. 3281. doi:10.1007/s11661-005-0002-x
[29] BHADESHIA, H. K. D. H.: Mater. Sci. Forum, *500/501*, 2005, p. 63. doi:10.4028/www.scientific.net/MSF.500-501.63
[30] KIM, D. H.—SPEER, J. G.—KIM, H. S.—DE COOMAN, B. C.: Metall. Mater. Trans. A, *40*, 2009, p. 2048. doi:10.1007/s11661-009-9891-4
[31] DAVENPORT, E. S.—BAIN, E. C.: Trans AIME, *90*, 1930, p. 117.
[32] KURDJUMOV, G. V.—MAKSIMOVA, O. P.: Dokl. Akad. Nauk SSSR, *61*, 1948, p. 83.
[33] RADCLIFFE, S. V.—ROLLASON, E. C.: J. Iron Steel Inst., *191*, 1959, p. 56.
[34] SUN, J.—LU, H.—KANG, M.: Metall. Mater. Trans. A, *23A*, 1992, p. 2483. doi:10.1007/BF02658052
[35] SCRUBY, C.—WADLEY, H.: J. Mater. Sci., *28*, 1993, p. 2501. doi:10.1007/BF01151686
[36] KANG, M.—ZHANG, M. X.—ZHU, M.: Acta Materialia, *54*, 2006, p. 2121. doi:10.1016/j.actamat.2005.12.036
[37] GARCIA DE ANDREAS, C.—CABALLERO, F. G.—CAPDEVILA, C.—ALVAREZ, L. F.: Materials Characterization, *48*, 2002, p. 101.
[38] CHUPATANAKUL, S.—NASH, P.: J. Mater. Sci., *41*, 2006, p. 4965. doi:10.1007/s10853-006-0127-3
[39] BHADESHIA, H. K. D. H.: Bainite in Steels. 2-nd ed. London, The Institute of Materials 2001.
[40] BERGNER, F.—KÖHLER, B.—POPP, K.: International Journal of Pressure Vessels and Piping, *55*, 1993, p. 251. doi:10.1016/0308-0161(93)90033-P